

Efficient Large-Scale Traffic Forecasting with Transformers: A Spatial Data Management Perspective

Yuchen Fang

University of Electronic Science and
Technology of China
fangyuchen@std.uestc.edu.cn

Yuxuan Liang

The Hong Kong University of Science
and Technology (Guangzhou)
yuxliang@outlook.com

Bo Hui

Auburn University
bzh0055@auburn.edu

Zezhi Shao

Institute of Computing Technology,
Chinese Academy of Sciences
shaozezhi@ict.ac.cn

Liwei Deng

University of Electronic Science and
Technology of China
deng_liwei@std.uestc.edu.cn

Xu Liu

National University of Singapore
liuxu@comp.nus.edu.sg

Xinke Jiang

Peking University
thinkerjiang@foxmail.com

Kai Zheng*

University of Electronic Science and
Technology of China
zhengkai@uestc.edu.cn

ABSTRACT

Road traffic forecasting is crucial in real-world intelligent transportation scenarios like traffic dispatching and path planning in city management and personal traveling. Spatio-temporal graph neural networks (STGNNs) stand out as the mainstream solution in this task. Nevertheless, the quadratic complexity of remarkable dynamic spatial modeling-based STGNNs has become the bottleneck over large-scale traffic data. From the spatial data management perspective, we present a novel Transformer framework called PatchSTG to efficiently and dynamically model spatial dependencies for large-scale traffic forecasting with interpretability and fidelity. Specifically, we design a novel irregular spatial patching to reduce the number of points involved in the dynamic calculation of Transformer. The irregular spatial patching first utilizes the leaf K-dimensional tree (KDTree) to recursively partition irregularly distributed traffic points into leaf nodes with a small capacity, and then merges leaf nodes belonging to the same subtree into occupancy-equalled and non-overlapped patches through padding and backtracking. Based on the patched data, depth and breadth attention are used interchangeably in the encoder to dynamically learn local and global spatial knowledge from points in a patch and points with the same index of patches. Experimental results on four real world large-scale traffic datasets show that our PatchSTG achieves train speed and memory utilization improvements up to 10 \times and 4 \times with the state-of-the-art performance.

*Corresponding author: Kai Zheng. He is with Yangtze Delta Region Institute (Quzhou), and School of Computer Science and Engineering, University of Electronic Science and Technology of China.

Permission to make digital or hard copies of all or part of this work for personal or classroom use is granted without fee provided that copies are not made or distributed for profit or commercial advantage and that copies bear this notice and the full citation on the first page. Copyrights for components of this work owned by others than the author(s) must be honored. Abstracting with credit is permitted. To copy otherwise, or republish, to post on servers or to redistribute to lists, requires prior specific permission and/or a fee. Request permissions from [permissions@acm.org](https://permissions.acm.org).

SIGKDD '25, August 3–7, 2025, Toronto, ON, Canada

© 2025 Copyright held by the owner/author(s). Publication rights licensed to ACM.
ACM ISBN 978-1-4503-XXXX-X/18/06...\$15.00
<https://doi.org/XXXXXXX.XXXXXXX>

CCS CONCEPTS

• **Computing methodologies** → **Neural networks**; • **Information systems** → **Spatial-temporal systems**.

KEYWORDS

traffic forecasting, Transformer, spatial data management

ACM Reference Format:

Yuchen Fang, Yuxuan Liang, Bo Hui, Zezhi Shao, Liwei Deng, Xu Liu, Xinke Jiang, and Kai Zheng. 2025. Efficient Large-Scale Traffic Forecasting with Transformers: A Spatial Data Management Perspective. In *Proceedings of the 31th ACM SIGKDD Conference on Knowledge Discovery and Data Mining (KDD '25)*, August 3–7, 2025, Toronto, Canada. ACM, New York, NY, USA, 11 pages. <https://doi.org/XXXXXXX.XXXXXXX>

1 INTRODUCTION

Road traffic data comprises multiple traffic time series collected from points where road sensors are deployed. Thus traffic time series are correlated in not only the temporal aspect but also spatial domain. Forecasting future road traffic through past data plays an essential role in many real world intelligent transportation applications. For instance, users on Map platforms can select the least time path in advance according to the predicted traffic [7, 33, 40, 41]. Likewise, on city management platforms [6], users can control the signal light to avoid congestion based on future traffic [10, 29, 53].

To accurately forecast future road traffic, countless algorithms have been proposed in past decades, ranging from statistical models [2] to data-driven methods [27]. In the beginning, temporal modeling methods like the recurrent neural network (RNN) and autoregressive integrated moving average (ARIMA) are used to learn the temporal evolution of the single traffic time series in traffic data [28, 46], yet ignore the spatial transmission between multiple traffic time series. Subsequently, spatio-temporal graph neural networks [26, 45, 55] are at the forefront of collaboratively capturing spatio-temporal dependencies.

However, the spatial correlation of traffic points is evolved over time and the fixed static graph in conventional spatio-temporal

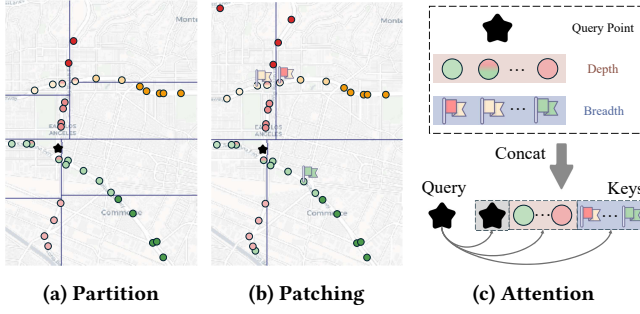


Figure 1: Sketch of our PatchSTG. We first partition the equilibrium number of points into small regions. Then we merge small regions into patches after padding points into regions where the maximum number of points has not been reached. Finally, we perform the depth and breadth attention on points in the same patch and points in other patches with the same index to capture local and global spatial knowledge.

graph neural networks can not reflect various correlations in different time stages. Therefore, dynamic spatial modeling technology has been focused as the mainstream research line in traffic forecasting [17], which aims to reveal spatial correlations of each time slice respectively and dynamically propagate spatial information. Considering the quadratic complexity in most dynamic spatial modeling methods, traffic forecasting is only performed at zone scale, which is opposite to the realistic traffic forecasting needs in a city with thousands of traffic points [43].

As shown in Table 1, three widely used dynamic spatial modeling paradigms (dot-product, linear, and low-rank) are illustrated in the attention form, *i.e.*, using query and key to dynamically calculate spatial correlations first and then propagating spatial information to the original value according to computed spatial correlations. Spatial correlations in dot-product-based methods such as D2STGNN [51] and STAEformer [39] should be calculated on each pair of points thus leading to unacceptable quadratic complexity in large-scale traffic forecasting. Despite linear-based BigST [20] and low-rank-based Airformer [37] being proposed to mitigate the high computation needs of dynamic spatial modeling in large-scale spatio-temporal forecasting, they still have some limitations. The drawback of linear-based [13, 20] is the lack of interpretability because spatial correlations can not be explicitly shown. For low-rank-based [12, 36], the blemish is a lack of fidelity, *i.e.*, crucial information cannot be guaranteed to remain in the reduced low-rank representations and thus results in a performance drop.

This work aims to reduce the computation needs of dynamic spatial modeling with high interpretability and without information loss in large-scale traffic forecasting by proposing an efficient Transformer framework called PatchSTG. The sketch of PatchSTG is illustrated in Figure 1 and the core goal of PatchSTG is to reduce the number of points involved in dynamic calculations like vision Transformers [44]. However, traffic points are irregularly distributed on roads, and thus simply splitting the same number of points into patches with equal size to reduce complexity in regular spatial data-based vision tasks is unsatisfactory in traffic forecasting. Inspired

Table 1: Four dynamic spatial modeling paradigms in traffic forecasting including previous dot-product, linear, low-rank, and our proposed patching. N , R , and d denote the number of traffic points, the number of points after cluster or sampling, and the number of model dimensions. In general, $R \ll N$ and $d \ll N$. Q , K , V , \bar{K} , and \bar{V} are query, key, value, reduced low-rank key, and reduced low-rank value in dynamic spatial modeling via attention form.

Paradigm	Dot-Product	Linear	Low-Rank	Patching
Complexity	$O(N^2d)$	$O(Nd^2)$	$O(NRd)$	$O(NRd)$
Formulation	$(QK^T)V$	$Q(K^TV)$	$(Q\bar{K}^T)\bar{V}^T$	$\sum_{i=1}^R \ (Q_{(i)}K_{(i)}^T)V_{(i)}\ $
Information Loss	✗	✗	✓	✗
Interpretability	✓	✗	✓	✓
Domain Knowledge	✓	✗	✗	✓

by the spatial data management algorithm KDTree (short for K-dimensional tree), we propose an irregular spatial patching method to split the same number of traffic points into patches with unequal size, which first uses the novel leaf KDTree to recursively partition all the traffic points into leaf nodes with the small capacity, and then merges leaf nodes belonging to the same subtree into occupancy-equal and non-overlapped patches through padding unfull leaf nodes and backtracking to the root node of subtrees. Finally, based on the patched data, PatchSTG first performs depth attention on points in a patch to learn local spatial knowledge and then conducts breadth attention on points in different patches but with the same index to efficiently aggregate multiple global knowledge. Notably, PatchSTG is interpretable and fidelity due to domain knowledge informed irregular spatial patching and non-compression dynamic spatial modeling.

In summary, we have made the following contributions:

- We present PatchSTG, a generic Transformer framework tailored for efficiently and effectively predicting large-scale traffic from the spatial data management perspective.
- To the best of our knowledge, we are the first to bridge the gap between KDTree and patching technique to evenly partition irregularly distributed traffic points with interpretability.
- PatchSTG performs the depth and breadth attention on points in a patch and points with the same index to efficiently learn dynamic local and global spatial knowledge with fidelity.
- Comprehensive experimental results on large-scale traffic datasets demonstrate that our PatchSTG achieves state-of-the-art performance and enjoys 4× memory reduction and 10× training speedup compared to dynamic spatial modeling baselines.

2 RELATED WORKS

2.1 Traffic Forecasting

Traffic forecasting has been a concern of research and industrial communities in past decades. Originally, the statistical-based vector autoregression (VAR) [2] and autoregressive integrated moving average (ARIMA) [28] are used to capture temporal dependencies. As

deep learning is splendid in many tasks, recurrent neural network-based methods [46] and temporal convolution network-based methods [16, 23] are proposed to improve traffic forecasting performance. To simultaneously extract spatio-temporal information, DCRNN [34] and STGCN [61] constructed a fixed adjacency matrix in graph neural networks [25, 62, 63] based on real-world distances to capture static spatial information for traffic forecasting. Subsequent techniques such as GWNET [59], AGCRN [1], MTGNN [58], METRO [4], STG-NCDE [3], and Localised AGCRN [9] have further improved forecasting accuracy through the data-driven fixed adjacency matrix. Nevertheless, most of them ignored the evolved spatial correlations of traffic. For calculating dynamic point-to-point spatial correlations, most approaches such as ASTGCN [17], GMAN [65], ST-GRAT [49], DMSTGCN [21], GMSDR [38], and etc. [24, 35, 39, 56, 64] applied the dot-product operation introduced by the attention mechanism on hidden representations with different periods. However, point-to-point dynamic models have brought the efficiency bottleneck into large-scale traffic forecasting. Despite efficient dynamic spatial modeling methods such as linear-based Lastjomer [13], BigST [20] and low-rank-based HUEST [47], SSTBAN [18] have been proposed to reduce the complexity, explicit spatial correlations are failed to report in linear-based methods and performance is restricted in low-rank-based methods compared with perceptron-based STID [50] and SimST [42] due to spatial reduction caused information loss. Therefore, we propose a novel efficient dynamic spatial modeling method PatchSTG, which is interpretable and fidelity.

2.2 Efficient Spatial Transformers

The quadratic complexity of dot-product attention has become the bottleneck in applying Transformers to learn spatial knowledge, thus efficient spatial Transformers have been researched in recent years. For regular spatial data such as images and videos, the same number of neighbored pixels can be simply merged into the same size patches such as ViT [8] and SwinTransformer [44] to decrease complexity by reducing points in the calculation. Different from regular spatial data, GraphTrans-ViT [22] and PatchGT [15] can only derive the overlapped and unbalanced patches through clustering algorithms. Luckily, STRN [36], FPT [48] and OctFormer [54] segmented images into patches with different sizes based on the semantic and distribution, which gave us the inspiration to use spatial data management algorithms for patching time-ordered irregular spatial data into balanced and non-overlapped patches.

3 PRELIMINARIES

Traffic Data. Traffic data is made up of multiple correlated time series collected from points where road sensors are deployed. The recorded time series of the specific traffic point n can be formulated as $x_n \in \mathbb{R}^H$, which contains traffic volume within H time slices. Therefore, traffic data that comprises time series on N points can be formed as a matrix $X \in \mathbb{R}^{H \times N}$, where x_n^h denotes the traffic flow of point n at time h .

Traffic Forecasting. In the traffic forecasting task, the common setting involves predicting future traffic features through historical values. Specifically, the goal of our paper is to forecast the future traffic flow for the next F time slices according to information from

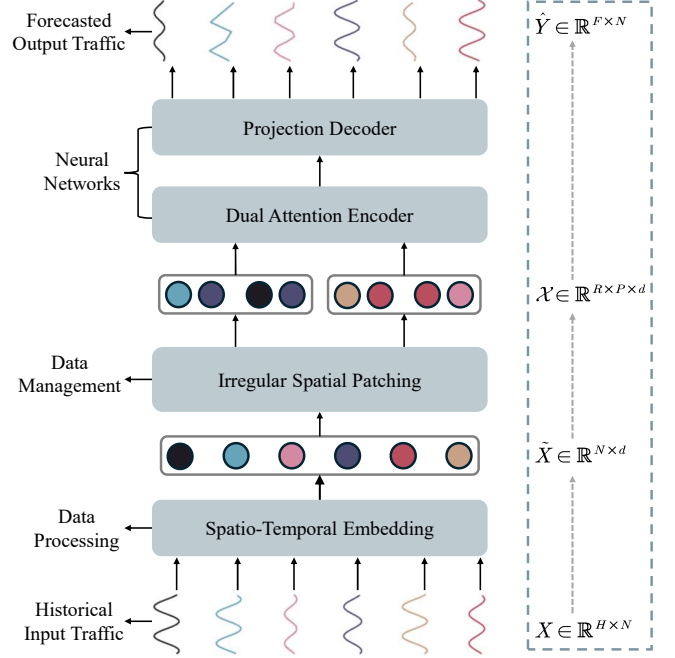


Figure 2: The workflow of our PatchSTG.

the preceding H time slices and the location of points.

$$\hat{Y} = f_{\theta}(X, Lat, Lng) \quad (1)$$

where $\hat{Y} \in \mathbb{R}^{F \times N}$ is the predicted traffic in the future, which will be used to compare with the ground truth $Y \in \mathbb{R}^{F \times N}$. $Lat \in \mathbb{R}^N$ and $Lng \in \mathbb{R}^N$ denote the real-world latitude and longitude of points. Moreover, the function $f_{\theta}(\cdot)$ indicates a data-driven forecasting model parameterized by θ .

4 METHODOLOGY

In this section, we present our PatchSTG framework, an effective and efficient solution designed for large-scale traffic forecasting. Figure 2 illustrates the overview of PatchSTG, which comprises four primary components: a spatio-temporal embedding module to preprocess traffic data into high-dimensional embeddings, an irregular spatial patching to split the same number of traffic points into patches, a dual attention encoder for extracting spatial information, and a projection decoder for predicting future values. We offer a detailed description of each component in the following.

4.1 Spatio-Temporal Embedding

Following previous works [30, 50], we adopt a fully-connected layer for each input traffic time series to transform their numerical traffic flow into high-dimensional embeddings. The detailed process of input traffic data $X \in \mathbb{R}^{H \times N}$ can be formulated as follows:

$$E = W_{(I)}X + b_{(I)} \quad (2)$$

where $W_{(I)} \in \mathbb{R}^{d_e \times H}$ and $b_{(I)} \in \mathbb{R}^{d_e}$ are learnable parameters of fully-connected layer. $E \in \mathbb{R}^{N \times d_e}$ is the projected embedding that contains the temporal evolution of traffic. Moreover, we take

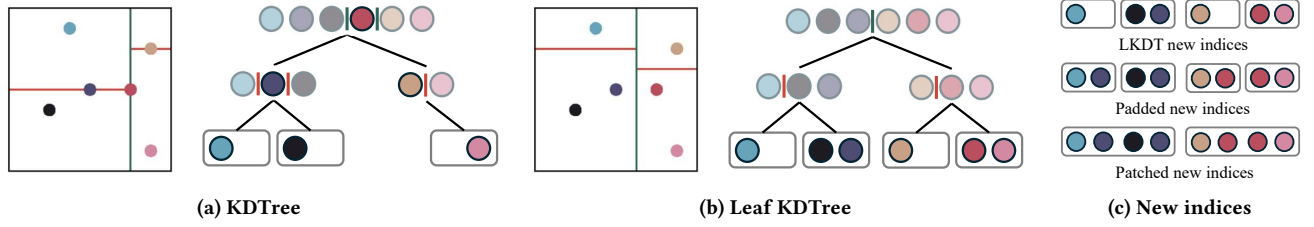


Figure 3: (a)-(b): left part draws the spatial partition using the original and leaf KDTree, and the right part is the corresponding tree. (c): KDT and LKDT are abbreviations of KDTree and leaf KDTree.

temporal daily patterns, temporal weekly patterns, and spatial heterogeneous patterns into consideration to improve the distinguishability of points followed by previous methods [39, 50]. For temporal aspect, day-of-week and timeslice-of-day patterns can be stored in the data-driven dictionary $W \in \mathbb{R}^{N_w \times d_w}$, $D \in \mathbb{R}^{N_d \times d_d}$, where N_w and N_d indicate the number of days in a week and the number of timeslices in a day. Therefore, we can use the last timeslice of all points as the index to extract corresponding day-of-week embedding $E_{(w)} \in \mathbb{R}^{N \times d_w}$ and timeslice-of-day embedding $E_{(d)} \in \mathbb{R}^{N \times d_d}$ from dictionaries. Similar to the temporal aspect, we utilize the learnable embedding $E_{(s)} \in \mathbb{R}^{N \times d_s}$ as identities to distinguish points in the dataset. Finally, we concatenate the above embeddings to derive the spatio-temporal embedding:

$$\tilde{X} = E || E_{(w)} || E_{(d)} || E_{(s)} \quad (3)$$

where $\tilde{X} \in \mathbb{R}^{N \times d}$ and $d = d_e + d_w + d_d + d_s$.

4.2 Irregular Spatial Patching

Motivation. Spatial propagation is indispensable in improving traffic forecasting performance evaluated by some methods [39, 57] in addition to spatial distinguishability. This is because vehicles moving on the road will bring real-time traffic changes in the source and destination areas. However, the quadratic complexity of remarkable dynamic spatial modeling methods is unacceptable under current computation resources. Fortunately, we find that spatial information in vision Transformers [44, 54] can be efficiently propagated on the patched input by reducing the number of points involved in attention. The difference between traffic and vision data is that pixels are regularly located in images but traffic points are irregularly distributed on roads, *i.e.*, the same number of pixels can be segmented into patches of the same size, but traffic points can not. Therefore, the main goal of our PatchSTG is to design a balanced and non-overlapped patching algorithm to reduce computation requirements of performing attention on irregular spatial data.

Leaf KDTree. As irregular spatial data management is essential for database, geoscience, etc., numerous spatial partitioning algorithms such as KDTree [52] and RTree [19] have been proposed. Considering the balance, non-overlapping, and efficiency requirements of partition, we take the simple yet effective KDTree into account to find a solution for evenly dividing irregular traffic data. As shown in Figure 3a, KDTree is a binary spatial tree that uses each internal node as a partitioning hyperplane to split points contained in the node between its two children excluding the hyperplane and is built by recursing on each child node after partitioning, until leaf

nodes are reached. Besides, the splitting hyperplane is determined by alternately chosen coordinate axes and the median point of the selected axis. In this paper, locations of latitude and longitude of traffic data are considered as axes to construct the tree. Unfortunately, as illustrated in Figure 3a, we find that hyperplane points in internal nodes of the conventional KDTree are not divided into leaf nodes and may result in irrelevant points being adjacent in the searching order. Therefore, we design a novel leaf KDTree as drawn in Figure 3b to enforce all points stored in leaf nodes, which utilizes the median value as the partitioning hyperplane for internal nodes with an even number of points, and the value between the median point and its left point as the partitioning hyperplane for internal nodes with an odd number of points. Moreover, from the illustration of our leaf KDTree in Figure 3b, we can observe that leaf nodes belonging to the same subtree maintain stronger spatial correlations based on their real-world closer distance, which provides the explainable backtracking for subsequent patching. After constructing leaf KDTree, we conduct the breath first searching on the tree to derive new indices of traffic points according to their searching order, which ensures that leaf nodes belonging to the same subtree are adjacent in the latest index. The entire process based on the latitude $Lat \in \mathbb{R}^N$, longitude $Lng \in \mathbb{R}^N$, and the capacity C of leaf nodes (leaf nodes in KDTree contain at most C points for a predetermined constant and $C = 2$ in Figure 3) can be formulated as follows:

$$idx = BFS(LKDT(Lat, Lng, C)) \quad (4)$$

where $idx \in \mathbb{R}^N$. $LKDT(\cdot)$ and $BFS(\cdot)$ denote the leaf KDTree construction and breath first search operation.

Padding. Despite leaf KDTree can provide an equilibrium partition, the number of traffic points N is not necessarily divisible by the capacity C , which leads to unfull leaf nodes as shown in Figure 3c. The inconsistent number destroys the application of patch-based efficient methods. Padding zeros or irrelevant points can mitigate the non-divisible issue yet decrease prediction performance. To make leaf nodes have equaled occupancy and non-self-repeating, we pad the points that are most similar to the unfull leaf nodes from other leaf nodes to reach the maximum capacity, which can confirm the non-overlap patches by the similar time series:

$$idx, \tilde{idx} = Query(LKDT(Lat, Lng, C), CosSim(X, X^T)) \quad (5)$$

where $Query(\cdot)$ denotes querying most similar points of each unfull leaf node through the Cosine similarity $CosSim(\cdot)$. idx and \tilde{idx} indicate locations should be padded in the new index and the corresponding original indices of queried points. Therefore, the padding

process can be formulated as follows:

$$\tilde{X} = \text{Pad}(\text{idx}, \tilde{\text{id}}x, \tilde{X}_{\tilde{\text{id}}x}) \quad (6)$$

where $\text{Pad}(\cdot)$ denotes padding queried neighbors into corresponding locations of new indices. Therefore, padded embedding $\tilde{X} \in \mathbb{R}^{M \times d}$ have M points and $M = C \times 2^{\lfloor \log(N) \rfloor - \log(C)} \geq N$.

Patching. Despite padded leaf nodes have the same number of points, directly using leaf nodes with a large capacity as patches will result in an unbalanced padding issue, *i.e.*, unfull leaf nodes may be padded by points similar to the same point. Recognizing that leaf nodes under the same subtree are strongly correlated and adjacent in new indices, we can first partition points into leaf nodes with a small capacity and then backtrack the tree from leaf nodes to root nodes of subtrees until meet the requirements that the number of the subtree is equal to the number of the pre-defined patch, which mitigates the unbalanced padding issue because unfull leaf nodes are mostly padded by points similar with different points. Concretely, let $P = C \times N_p$ indicate the number of points in a patch and R denotes the number of patches, where N_p is a hyper-parameter that determines how many leaf nodes in a subtree and $M = R \times P$. Notably, N_p can only be a power of 2 because only leaf nodes that belong to the same subtree have strong spatial locality and our leaf KDTree is a binary tree.

After our balanced and non-overlapped spatial patching, the padded embedding \tilde{X} is transformed into a new representation $\mathcal{X} \in \mathbb{R}^{R \times P \times d}$ as the input of the following neural networks.

4.3 Dual Attention Encoder

In this section, we present the dual attention encoder to dynamically capture spatial dependencies. For the patched input $\mathcal{X} \in \mathbb{R}^{R \times P \times d}$, R points in the first dimension can be seen as the root nodes of subtrees and P points in the second dimension can be seen points in the subtree. Therefore, PatchSTG first uses the depth attention on each patch to dynamically extract local spatial information because points in a subtree have stronger correlations. Moreover, as global dependencies are equally essential to the local information in traffic prediction [13], breadth attention is then adopted on the patch level to learn lossless global knowledge because each point in a root node of the subtree can receive information from points with the same index in other root nodes and these points are mixed with local information after previous depth attention. The dual attention can be interchangeably stacked L layers in the encoder, thus we describe the process of l -th layer in the following for simplicity.

Depth Attention. Depth attention is the multi-head scaled dot-product attention, which is used to capture local spatial information in patches. As shown in Figure 4, the query, key, and value are first derived by using learnable linear transformations on the input, which can be formulated as follows:

$$\begin{aligned} Q_{(P)_i}^{(l)} &= W_{(Q)_i}^{(l)} \mathcal{X}^{(l-1)} \\ K_{(P)_i}^{(l)} &= W_{(K)_i}^{(l)} \mathcal{X}^{(l-1)} \\ V_{(P)_i}^{(l)} &= W_{(V)_i}^{(l)} \mathcal{X}^{(l-1)} \end{aligned} \quad (7)$$

where $1 \leq i \leq o$ in our multi-head setting. $Q_{(P)_i}^{(l)}, K_{(P)_i}^{(l)}, V_{(P)_i}^{(l)} \in \mathbb{R}^{R \times P \times \frac{d}{o}}$ indicate the query, key, and value of each head in l -th

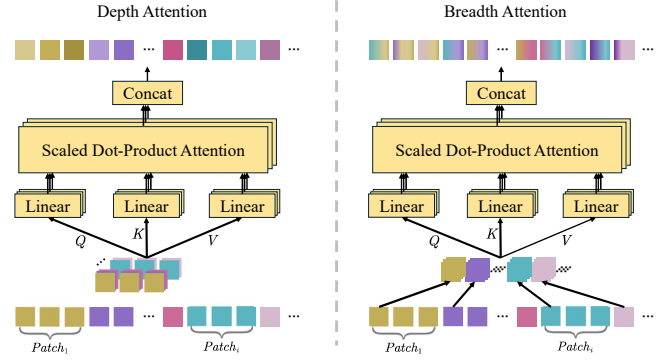


Figure 4: Structure of depth and breadth attention.

layer, and $W_{(Q)_i}^{(l)}, W_{(K)_i}^{(l)}, W_{(V)_i}^{(l)} \in \mathbb{R}^{d \times \frac{d}{o}}$ are learnable parameters. Notably $\mathcal{X}^{(0)} = \mathcal{X}$ for the encoder. Then we utilize the query and key to dynamically compute point correlations (shape is $\mathbb{R}^{R \times P \times P}$) of each patch, and leverage it to attend spatial information:

$$A_{(P)_i}^{(l)} = \text{Softmax}\left(\frac{Q_{(P)_i}^{(l)} K_{(P)_i}^{(l)T}}{\sqrt{d/o}}\right) V_{(P)_i}^{(l)} \quad (8)$$

where $\text{Softmax}(\cdot)$ normalizes correlations. Finally, multi-head results of the l -th layer are concatenated:

$$\tilde{\mathcal{X}}^{(l)} = (A_{(P)_1}^{(l)} || \dots || A_{(P)_o}^{(l)}) W_{(O)}^{(l)} \quad (9)$$

where $W_{(O)}^{(l)} \in \mathbb{R}^{d \times d}$ denotes the learnable parameter.

Breadth Attention. Breadth attention is also the multi-head scaled dot-product attention, which is used to learn global spatial knowledge at the patch level. Similarly, the query, key, and value $Q_{(R)_i}^{(l)}, K_{(R)_i}^{(l)}, V_{(R)_i}^{(l)} \in \mathbb{R}^{P \times R \times \frac{d}{o}}$ are first derived by using learnable linear transformations on the output of depth attention. Then query and key are used to dynamically compute patch correlations (shape is $\mathbb{R}^{P \times R \times R}$) of each index in patches. Finally, the output of the l -th layer $\mathcal{X}^{(l)} \in \mathbb{R}^{R \times P \times d}$ is derived by using the calculated correlations to attend global information.

4.4 Projection Decoder

In this section, we aim to predict the future traffic through the spatial information interacted output $\mathcal{X}^{(L)} \in \mathbb{R}^{R \times P \times d}$ of the dual attention encoder. We first unpatch the output to $\tilde{\mathcal{X}}^{(L)} \in \mathbb{R}^{M \times d}$ through performing depth first search operation on each root node, and unpad leaf nodes to consist with the input shape and index:

$$\tilde{Y}_{\tilde{\text{id}}x} = \text{UnPad}(\text{idx}, \tilde{\mathcal{X}}^{(L)}) \quad (10)$$

where $\text{UnPad}(\cdot)$ denotes removing points on the unpadded locations and $\tilde{Y} \in \mathbb{R}^{N \times d}$ is the representation with original index. Finally, a fully connected layer is adopted to project the historical representation into the future:

$$\hat{Y} = W_{(D)} \tilde{Y} + b_{(D)} \quad (11)$$

where $W_{(D)} \in \mathbb{R}^{F \times d}$, $b_{(D)} \in \mathbb{R}^F$ are learnable parameters and $\hat{Y} \in \mathbb{R}^{F \times N}$ indicates predicted traffic. During the training stage, we

use \hat{Y} and Y to compute L1 loss as the objective function to guide the learning of PatchSTG.

4.5 Complexity Analysis

The leaf KDTree takes $O(N \log(N))$ complexity to construct the balanced binary tree based on the median hyperplane [5], which can be quickly done in the pre-processing stage. In the dual attention encoder, the cost of depth and breadth attention is respectively $O(RP^2d)$ and $O(PR^2d)$. Therefore, the dominant complexity of PatchSTG is $O(\max(P, R)Md)$, which requires less time than quadratic dynamic spatial modeling methods because $P \ll N$, $R \ll N$, and $M \approx N$ in PatchSTG.

Table 2: Dataset statistics.

Datasets	#Points	#Samples	#TimeSlices	Timespan
SD	716	25M	35040	01/01/2019-12/31/2019
GBA	2352	82M	35040	01/01/2019-12/31/2019
GLA	3834	134M	35040	01/01/2019-12/31/2019
CA	8600	301M	35040	01/01/2019-12/31/2019

5 EXPERIMENTS

The goal of this section is to address the following five pivotal research questions by conducting comprehensive experiments on four large-scale traffic datasets.

- **RQ1:** How does PatchSTG perform when compared to current approaches in large-scale traffic forecasting?
- **RQ2:** What contributions do the main components of PatchSTG?
- **RQ3:** How efficient is PatchSTG in large-scale datasets?
- **RQ4:** Does PatchSTG output reasonable correlations?
- **RQ5:** How do the essential hyper-parameters impact PatchSTG?

5.1 Experimental Setup

5.1.1 Datasets. We conduct experiments on four large-scale datasets SD, GBA, GLA, and CA as introduced in LargeST [43]. Following previous settings, we not only chronologically split each dataset into train, validation, and test sets with a ratio of 6:2:2 but also utilize continuous 24 time slices as samples to perform traffic forecasting with the historical 12 time slices as the input and the future 12 time slices as the output. Detailed statistics of these datasets are shown in Table 2.

5.1.2 Baselines. We compare 10 advanced baselines in this paper with our PatchSTG. (i) The non-spatial modeling-based STID [50], which uses identity spatio-temporal embeddings in fully-connected layers to forecast traffic. (ii) In the category of static spatial-based methods, we select GWNET [59], AGCRN [1], STGODE [14], and RPMixer [60]. They combine various static GNNs with temporal networks for traffic forecasting. (iii) Baselines in the dynamic spatial-based category include, DSTAGNN [31], D2STGNN [51], DGCRN [32], low-rank STWave [11], and linear BigST [20]. They dynamically reveal spatial correlations at different time periods for traffic forecasting.

5.1.3 Evaluation Metrics. We utilize diverse evaluation criteria from performance and efficiency aspects for a comprehensive comparison. For the performance aspect: we utilize three commonly

adopted numerical metrics to assess the performance of predicted traffic time series, *i.e.*, mean absolute error (MAE), root mean squared error (RMSE), and mean absolute percentage error (MAPE). For the efficiency aspect: the measurement of the model’s efficiency is based on the wall-clock time, and the memory needs of models are revealed by the batch size in the training phase.

5.1.4 Implementation Details. During training, PatchSTG is optimized by the AdamW optimizer with a learning rate of 0.002 and weight decay of 0.0001, and the training epoch is set to 50 for all datasets. Moreover, the learning rate is halved at 2, 35, and 40 epochs. To better reproduce our model, we summarize all the default hyper-parameters as follows. The dimension of input projection in SD, GBA, GLA, and CA datasets is set to 128, 128, 64, and 64. The dimension of day-of-week embedding, timeslice-of-day embedding, and spatial embedding is all set to 32. The number of segmented patches of CA, GLA, GBA, and SD is set to 512, 64, 16, and 16. The number of points in a leaf node is set as 3, 2, 2, and 2 for CA, GLA, GBA, and SD. The number of attention layers is set to 5. Besides, all the experiments are implemented in PyTorch with the NVIDIA RTX A6000 48GB GPU. The source code of PatchSTG is available at: <https://github.com/LMissher/PatchSTG>.

5.2 Performance Comparisons (RQ1)

Table 3 showcases the MAE, RMSE, and MAPE of traffic forecasting across all methods on four large-scale datasets except for failure to run with the smallest batch size of 1. The performance on the horizon 3, horizon 6, horizon 12, and the average of the whole 12 horizons are reported. To ensure a fair comparison, we follow official configurations of baselines, with the only adjustment of fixes input length to 12. Therefore baselines in our paper may show slight variations compared to the original results.

Advantages of Distinguishability. Among the baselines concerned, identity embedding-based non-spatial STID, shows a significant lead over spatial modeling methods on larger datasets such as the CA dataset. This phenomenon underscores the advantages of learning heterogeneous representations of different points to avoid over-smoothing in spatial message passing.

Advantages of Dynamic Spatial Modeling. As shown in Table 3, D2STGNN exhibits remarkable superiority, especially on the SD dataset when compared to non-spatial and static spatial-based methods. This appearance is owing to the dynamic spatial modeling. Despite point-to-point D2STGNN achieving great performance in small-scale datasets, it is still limited by the quadratic complexity in large-scale GLA and CA datasets.

Advantages of Explicit Spatial Aggregation. In large-scale datasets, in contrast to linear-based efficient dynamic spatial modeling method BigST, low rank-based STWave demonstrates clear advantages on all datasets under spatial reduction caused information loss, attributed to the implicit spatial correlations in linear-based methods are failed to correctly normalize.

Consistent Performance Superiority. Drawing on the aforementioned components and our irregular spatial patching, we introduce PatchSTG, an efficient Transformer framework that achieves state-of-the-art performance on all datasets as evidenced in Table 3.

Table 3: Large-scale traffic forecasting performance comparison of our PatchSTG and baselines. Redfont indicates the best performance and bluefont denotes the second best performance.

Datasets	Methods	Horizon 3			Horizon 6			Horizon 12			Average		
		MAE	RMSE	MAPE (%)	MAE	RMSE	MAPE (%)	MAE	RMSE	MAPE (%)	MAE	RMSE	MAPE (%)
SD	STID	15.15	25.29	9.82	17.95	30.39	11.93	21.82	38.63	15.09	17.86	31.00	11.94
	GWNET	15.24	25.13	9.86	17.74	29.51	11.70	21.56	36.82	15.13	17.74	29.62	11.88
	AGCRN	15.71	27.85	11.48	18.06	31.51	13.06	21.86	39.44	16.52	18.09	32.01	13.28
	STGODE	16.75	28.04	11.00	19.71	33.56	13.16	23.67	42.12	16.58	19.55	33.57	13.22
	RPMixer	18.54	30.33	11.81	24.55	40.04	16.51	35.90	58.31	27.67	25.25	42.56	17.64
	DSTAGNN	18.13	28.96	11.38	21.71	34.44	13.93	27.51	43.95	19.34	21.82	34.68	14.40
	D2STGNN	14.92	24.95	9.56	17.52	29.24	11.36	22.62	37.14	14.86	17.85	29.51	11.54
	DGCRN	15.34	25.35	10.01	18.05	30.06	11.90	22.06	37.51	15.27	18.02	30.09	12.07
	STWave	15.80	25.89	10.34	18.18	30.03	11.96	21.98	36.99	15.30	18.22	30.12	12.20
	BigST	16.42	26.99	10.86	18.88	31.60	13.24	23.00	38.59	15.92	18.80	31.73	12.91
	PatchSTG	14.53	24.34	9.22	16.86	28.63	11.11	20.66	36.27	14.72	16.90	29.27	11.23
GBA	STID	17.36	29.39	13.28	20.45	34.51	16.03	24.38	41.33	19.90	20.22	34.61	15.91
	GWNET	17.85	29.12	13.92	21.11	33.69	17.79	25.58	40.19	23.48	20.91	33.41	17.66
	AGCRN	18.31	30.24	14.27	21.27	34.72	16.89	24.85	40.18	20.80	21.01	34.25	16.90
	STGODE	18.84	30.51	15.43	22.04	35.61	18.42	26.22	42.90	22.83	21.79	35.37	18.26
	RPMixer	20.31	33.34	15.64	26.95	44.02	22.75	39.66	66.44	37.35	27.77	47.72	23.87
	DSTAGNN	19.73	31.39	15.42	24.21	37.70	20.99	30.12	46.40	28.16	23.82	37.29	20.16
	D2STGNN	17.54	28.94	12.12	20.92	33.92	14.89	25.48	40.99	19.83	20.71	33.65	15.04
	DGCRN	18.02	29.49	14.13	21.08	34.03	16.94	25.25	40.63	21.15	20.91	33.83	16.88
	STWave	17.95	29.42	13.01	20.99	34.01	15.62	24.96	40.31	20.08	20.81	33.77	15.76
	BigST	18.70	30.27	15.55	22.21	35.33	18.54	26.98	42.73	23.68	21.95	35.54	18.50
	PatchSTG	16.81	28.71	12.25	19.68	33.09	14.51	23.49	39.23	18.93	19.50	33.16	14.64
GLA	STID	16.54	27.73	10.00	19.98	34.23	12.38	24.29	42.50	16.02	19.76	34.56	12.41
	GWNET	17.28	27.68	10.18	21.31	33.70	13.02	26.99	42.51	17.64	21.20	33.58	13.18
	AGCRN	17.27	29.70	10.78	20.38	34.82	12.70	24.59	42.59	16.03	20.25	34.84	12.87
	STGODE	18.10	30.02	11.18	21.71	36.46	13.64	26.45	45.09	17.60	21.49	36.14	13.72
	RPMixer	19.94	32.54	11.53	27.10	44.87	16.58	40.13	69.11	27.93	27.87	48.96	17.66
	DSTAGNN	19.49	31.08	11.50	24.27	38.43	15.24	30.92	48.52	20.45	24.13	38.15	15.07
	STWave	17.48	28.05	10.06	21.08	33.58	12.56	25.82	41.28	16.51	20.96	33.48	12.70
	BigST	18.38	29.40	11.68	22.22	35.53	14.48	27.98	44.74	19.65	22.08	36.00	14.57
	PatchSTG	15.84	26.34	9.27	19.06	31.85	11.30	23.32	39.64	14.60	18.96	32.33	11.44
CA	STID	15.51	26.23	11.26	18.53	31.56	13.82	22.63	39.37	17.59	18.41	32.00	13.82
	GWNET	17.14	27.81	12.62	21.68	34.16	17.14	28.58	44.13	24.24	21.72	34.20	17.40
	STGODE	17.57	29.91	13.91	20.98	36.62	16.88	25.46	45.99	21.00	20.77	36.60	16.80
	RPMixer	18.18	30.49	12.86	24.33	41.38	18.34	35.74	62.12	30.38	25.07	44.75	19.47
	STWave	16.77	26.98	12.20	18.97	30.69	14.40	25.36	38.77	19.01	19.69	31.58	14.58
	BigST	17.15	27.92	13.03	20.44	33.16	15.87	25.49	41.09	20.97	20.32	33.45	15.91
	PatchSTG	14.69	24.82	10.51	17.41	29.43	12.83	21.20	36.13	16.00	17.35	29.79	12.79

5.3 Ablation Study (RQ2)

In this section, ablation experiments are conducted on four datasets using four variants of PatchSTG to address RQ2. These four variants are listed below:

- "w/o FGCC": PatchSTG fuse all points in the same patch into a single patch point during the breadth attention.
- "w/o Depth": PatchSTG removes the depth attention and only global spatial correlations are modeled.
- "w/o Breadth": PatchSTG removes the breadth attention and only local spatial correlations are modeled.
- "w/ PadDis": PatchSTG pads points with closest distance into unfull patches.

- "w/o PadSim": This variant only pads zero constants but not other points into unfull leaf nodes.
- "w/ METIS": This variant uses the balanced graph partition algorithm METIS to replace our Leaf KDTree.
- "w/ KMeans": This variant utilizes the unbalanced clustering algorithm KMeans to substitute our Leaf KDTree.
- "w/o LKDT": PatchSTG no longer equips the leaf KDTree, *i.e.*, dual attention is conducted on the original input.

According to the results illustrated in Table 4, the following observations can be found.

Benefits Brought by KDTree. Experimental results of "w/o LKDT" on all datasets show a huge drop in prediction performance,

Table 4: Ablation study of PatchSTG on average results of large-scale traffic datasets. Bold: best performance.

Dataset	SD			GBA			GLA			CA		
Metric	MAE	RMSE	MAPE (%)	MAE	RMSE	MAPE (%)	MAE	RMSE	MAPE (%)	MAE	RMSE	MAPE (%)
w/o FGGC	17.37	29.44	11.45	19.72	33.28	15.51	19.49	32.95	11.69	17.63	30.04	13.05
w/o Depth	17.18	29.91	11.28	19.63	33.33	15.11	19.38	33.05	11.73	17.68	30.32	13.09
w/o Breadth	17.70	30.55	11.46	19.90	33.44	15.28	19.65	33.66	12.18	18.04	30.74	13.17
w/ PadDis	17.02	29.42	11.34	19.60	33.32	15.03	19.17	32.80	11.63	17.50	30.14	13.00
w/o PadSim	17.00	29.43	11.25	19.57	33.34	15.32	19.57	33.18	11.80	17.87	30.52	13.11
w/ METIS	18.00	30.69	11.72	19.91	33.38	15.16	19.63	33.57	11.86	18.02	30.53	13.02
w/ KMeans	18.07	30.76	11.87	20.16	33.93	15.87	19.85	34.07	11.90	18.26	31.08	13.05
w/o LKDT	17.58	29.38	11.45	20.14	34.18	15.91	19.88	34.47	12.31	18.27	30.97	13.00
PatchSTG	16.90	29.27	11.23	19.50	33.16	14.64	18.96	32.33	11.44	17.35	29.79	12.79

Table 5: Efficiency comparisons on large-scale traffic datasets. BS: batch size. Train: training time (in seconds) per epoch. Infer: inference time (in seconds). Total: total training time (in hours). Note that $Total = Train \times Epochs$ and - indicates out of memory.

Methods	SD				GBA				GLA				CA			
	BS	Train	Infer	Total	BS	Train	Infer	Total	BS	Train	Infer	Total	BS	Train	Infer	Total
DSTAGNN	64	240	23	7	27	1959	171	53	10	5241	467	120	-	-	-	-
D2STGNN	45	563	69	14	4	5885	796	148	-	-	-	-	-	-	-	-
DGCRN	64	430	76	14	12	4461	605	138	-	-	-	-	-	-	-	-
STWave	64	259	33	7	36	926	120	26	22	1483	179	41	8	3641	437	101
PatchSTG	64	64	6	1	64	262	30	4	64	295	27	4	32	981	93	14
Improvements	0×	3.8×	3.8×	7×	1.8×	1.8×	4×	6.5×	2.9×	5×	6.6×	10×	4×	3.7×	4.7×	7.2×

recommending that the most important in PatchSTG is not dynamically modeling spatial dependencies on irrelevant points in the patch but passing spatial messages on adjacent points in the patch. Moreover, the performance of STID and "w/o LKDT" on the GLA dataset further verifies that our leaf KDTree is the key component to model local spatial information. Besides, we test some methods that can also segment the traffic data into multiple patches. The conventional graph cluster methods such as KMeans not only achieve poor performance as "w/ KMeans" but also fail to derive balanced patching (the maximum and minimum patch size of KMeans on the SD dataset is 96 and 6). Though the graph partition method METIS can approximately segment traffic data into balanced patches, it cannot derive balance padded non-overlap patches because the recursive merge operation in our leaf KDTree is not supported, and thus performs badly as "w/ METIS".

Effectiveness of Non-Overlap Padding. The experiments of "w/ PadDis" and "w/o PadSim" reflect that, in all datasets, replacing similar points with zeros or neighbored points to pad unfull leaf nodes results in a drop in performance. This finding underscores the effectiveness of our non-overlap padding from the temporal view and backtracking merging for balanced padding.

Effectiveness of Dual Attention. As observed by the decreased performance in "w/o Depth," depth attention is essential in PatchSTG to capture local spatial dependencies. Similar to the local information, global spatial interactions are also indispensable in spatial modeling as the performance drop of "w/o Breadth". Besides, compared with the "w/o FGGC" performance, our non-fused fine-grained global modeling achieves better results because it preserves diverse global information and thus our PatchSTG is fidelity.

5.4 Efficiency Comparisons (RQ3)

To evaluate the efficiency of our PatchSTG, we present the training speed, inference speed, and batch size comparisons among our PatchSTG and previous dynamic spatial modeling methods with explicit spatial correlations, including DSTAGNN, D2STGNN, DGCRN, and STWave. As depicted in Table 5, PatchSTG attains the fastest speed and boasts the most efficient GPU memory utilization across all datasets, especially achieving up to 10× and 4× improvements in speed and memory on large-scale GLA and CA datasets. While low-rank-based STWave also excels other methods in speed on large-scale datasets, the worse performance of STWave on small datasets compared to quadratic complexity-based DSTAGNN suggests that low-rank-based methods are less general than our PatchSTG under different settings.

5.5 Visualization (RQ4)

Interpretability. To verify the interpretability of our PatchSTG, we visualize the evenly segmented GLA dataset using our leaf KDTree in Figure 5. We can observe that the real-world adjacent points are obviously divided into the same leaf node to maintain spatial locality, which can give explainable spatial partition compared with low-rank-based dynamic spatial modeling methods. Moreover, our PatchSTG can explicitly show the learned local and global spatial correlations corresponding to their real-world locations on the segmented map, which is interpretable compared with linear-based dynamic spatial modeling methods.

Fidelity. To show our framework of learning global spatial knowledge without information loss, we conduct a case study on the GLA dataset, *i.e.*, we visualize the learned patch correlations of

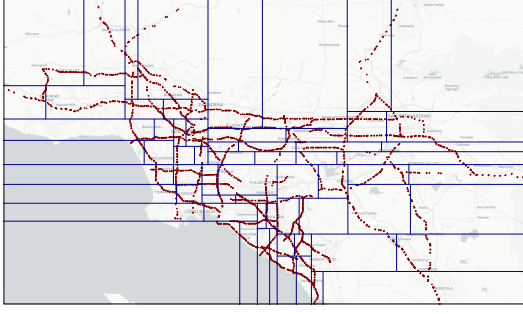


Figure 5: Leaf KDTree on the GLA dataset.

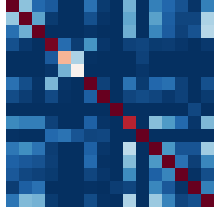
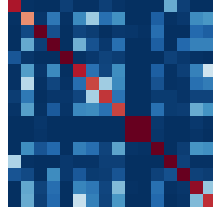
(a) Correlations on 23th(b) Correlations on 56th

Figure 6: Learned patch-level correlations.

points with indices 23 and 56 in the patch. As shown in Figure 6, the global correlations learned by the breadth attention are diverse for different indices in the patch, which follows the heterogeneity of traffic points. Therefore, our PatchSTG is fidelity compared with low-rank-based methods because they can only reflect same patch correlations for all points in the patch.

5.6 Hyper-parameter Study (RQ5)

Figure 7 draws the impact of hyper-parameters on the representative GBA and CA datasets. We search the number of attention layers and the number of input fully-connected dimensions from a search space of $[1, 3, 5, 7]$ and $[32, 64, 128, 256]$. First, the performance of PatchSTG improves as the layers of the encoder increase and tends to be best when there are 5 layers. Second, when the number of input dimensions is 64 and 128 on GBA and CA datasets, PatchSTG achieves the best performance. We can observe that the small model is enough to learn spatio-temporal knowledge in large-scale datasets due to rich patterns in big data.

Moreover, we search the number of patches from a search space of $[8, 16, 32, 64, 128, 256, 512]$ as shown in Figure 8. PatchSTG with 16, 16, 64, and 512 patches can achieve the best performance on SD, GBA, GLA, and CA datasets, which points out that the number of patches is positively correlated with the size of the dataset.

6 CONCLUSIONS

In this paper, we introduce a novel efficient Transformer framework PatchSTG from the spatial data management perspective for large-scale traffic forecasting. PatchSTG first utilizes the leaf KDTree to recursively partition the equilibrium number of irregular traffic points into leaf nodes with interpretability. Then PatchSTG patches

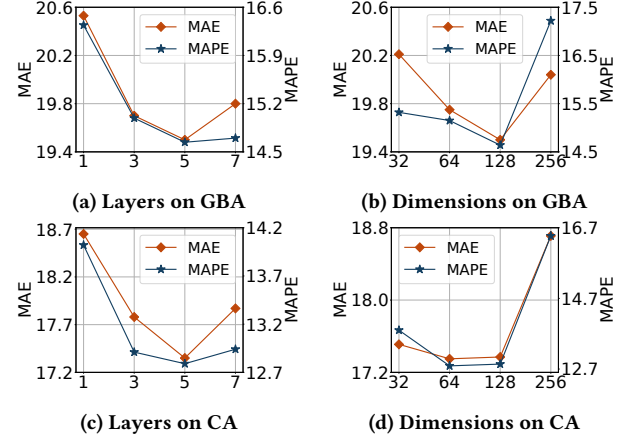


Figure 7: Hyper-parameter study.

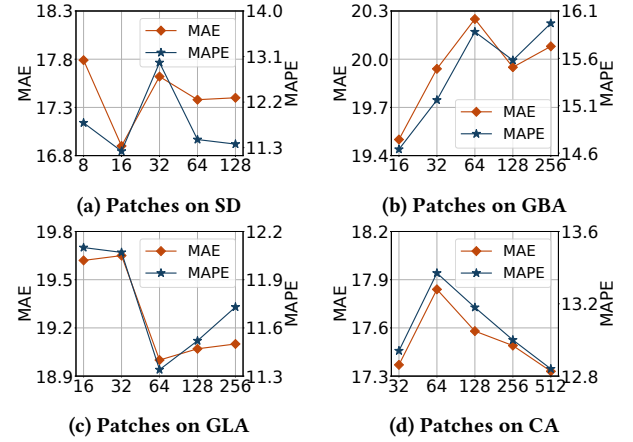


Figure 8: The influence of changing the number of patches.

leaf nodes with close distance together through backtracking after padding. Finally, PatchSTG stacks the depth and breadth attention in the encoder interchangeably to efficiently and dynamically capture spatial information from the patched data with fidelity. Experimental results on four large-scale benchmark datasets demonstrate the superior performance of PatchSTG against 10 baselines. We will extend PatchSTG to other spatio-temporal tasks in the future, such as national air quality prediction.

ACKNOWLEDGMENTS

This work is partially supported by NSFC (No. 62472068), Shenzhen Municipal Science and Technology R&D Funding Basic Research Program (JCYJ20210324133607021), and Municipal Government of Quzhou under Grant (2023D044), and Key Laboratory of Data Intelligence and Cognitive Computing, Longhua District, Shenzhen. This work is also supported by the National Natural Science Foundation of China (No. 62402414), the Guangzhou Industrial Information and Intelligent Key Laboratory Project (No. 2024A03J0628), and Guangdong Provincial Key Lab of Integrated Communication, Sensing and Computation for Ubiquitous Internet of Things (No. 2023B1212010007).

REFERENCES

- [1] Lei Bai, Lina Yao, Can Li, Xianzhi Wang, and Can Wang. 2020. Adaptive graph convolutional recurrent network for traffic forecasting. In *Proceedings of NeurIPS*. 17804–17815.
- [2] Srinivasa Ravi Chandra and Haitham Al-Deek. 2009. Predictions of freeway traffic speeds and volumes using vector autoregressive models. *Journal of Intelligent Transportation Systems* (2009), 53–72.
- [3] Jeongwhan Choi, Hwangyong Choi, Jeehyun Hwang, and Noseong Park. 2022. Graph neural controlled differential equations for traffic forecasting. In *Proceedings of AAAI*. 6367–6374.
- [4] Yue Cui, Kai Zheng, Dingshan Cui, Jiandong Xie, Liwei Deng, Feiteng Huang, and Xiaofang Zhou. 2021. METRO: a generic graph neural network framework for multivariate time series forecasting. *Proceedings of the VLDB Endowment* (2021), 224–236.
- [5] Mark De Berg, Otfried Cheong, Marc Van Kreveld, and Mark Overmars. 2008. Orthogonal range searching: Querying a database. *Computational Geometry: Algorithms and Applications* (2008), 95–120.
- [6] Liwei Deng, Tianfu Wang, Yan Zhao, and Kai Zheng. 2024. MILLION: A General Multi-Objective Framework with Controllable Risk for Portfolio Management. *arXiv preprint arXiv:2412.03038* (2024).
- [7] Liwei Deng, Yan Zhao, Yue Cui, Yuyang Xia, Jin Chen, and Kai Zheng. 2024. Task Recommendation in Spatial Crowdsourcing: A Trade-Off Between Diversity and Coverage. In *Proceedings of ICDE*. 276–288.
- [8] Alexey Dosovitskiy, Lucas Beyer, Alexander Kolesnikov, Dirk Weissenborn, Xi-aohua Zhai, Thomas Unterthiner, Mostafa Dehghani, Matthias Minderer, Georg Heigold, Sylvain Gelly, et al. 2020. An Image is Worth 16x16 Words: Transformers for Image Recognition at Scale. In *Proceedings of ICLR*. 1–22.
- [9] Wenying Duan, Xiaoxi He, Zimu Zhou, Lothar Thiele, and Hong Rao. 2023. Localised adaptive spatial-temporal graph neural network. In *Proceedings of SIGKDD*. 448–458.
- [10] Yuchen Fang, Haiyong Luo, Fang Zhao, Poly ZH Sun, Yanjun Qin, Liang Zeng, Bo Hui, and Chenxing Wang. 2024. CDGNet: A Cross-Time Dynamic Graph-Based Deep Learning Model for Vehicle-Based Traffic Speed Forecasting. *IEEE Transactions on Intelligent Vehicles* (2024).
- [11] Yuchen Fang, Yanjun Qin, Haiyong Luo, Fang Zhao, Bingbing Xu, Liang Zeng, and Chenxing Wang. 2023. When spatio-temporal meet wavelets: Disentangled traffic forecasting via efficient spectral graph attention networks. In *Proceedings of ICDE*. 517–529.
- [12] Yuchen Fang, Yanjun Qin, Haiyong Luo, Fang Zhao, and Kai Zheng. 2023. STWave+: A Multi-Scale Efficient Spectral Graph Attention Network With Long-Term Trends for Disentangled Traffic Flow Forecasting. *IEEE Transactions on Knowledge and Data Engineering* (2023), 2671–2685.
- [13] Yuchen Fang, Fang Zhao, Yanjun Qin, Haiyong Luo, and Chenxing Wang. 2022. Learning all dynamics: Traffic forecasting via locality-aware spatio-temporal joint transformer. *IEEE Transactions on Intelligent Transportation Systems* (2022), 23433–23446.
- [14] Zheng Fang, Qingqing Long, Guojie Song, and Kunqing Xie. 2021. Spatial-temporal graph ode networks for traffic flow forecasting. In *Proceedings of SIGKDD*. 364–373.
- [15] Han Gao, Xu Han, Jiaoyang Huang, Jian-Xun Wang, and Liping Liu. 2022. Patchgt: Transformer over non-trainable clusters for learning graph representations. In *Proceedings of LoG*. 1–27.
- [16] Ge Guo, Wei Yuan, Jinyuan Liu, Yisheng Lv, and Wei Liu. 2021. Traffic forecasting via dilated temporal convolution with peak-sensitive loss. *IEEE Intelligent Transportation Systems Magazine* (2021), 48–57.
- [17] Shengnan Guo, Youfang Lin, Ning Feng, Chao Song, and Huaiyu Wan. 2019. Attention based spatial-temporal graph convolutional networks for traffic flow forecasting. In *Proceedings of AAAI*. 922–929.
- [18] Shengnan Guo, Youfang Lin, Letian Gong, Chenyu Wang, Zeyu Zhou, Zekai Shen, Yiheng Huang, and Huaiyu Wan. 2023. Self-supervised spatial-temporal bottleneck attentive network for efficient long-term traffic forecasting. In *Proceedings of ICDE*. 1585–1596.
- [19] Antonin Guttman. 1984. R-trees: A dynamic index structure for spatial searching. In *Proceedings of SIGMOD*. 47–57.
- [20] Jindong Han, Weijia Zhang, Hao Liu, Tao Tao, Naiqiang Tan, and Hui Xiong. 2024. BigST: Linear Complexity Spatio-Temporal Graph Neural Network for Traffic Forecasting on Large-Scale Road Networks. *Proceedings of VLDB* (2024), 1081–1090.
- [21] Liangzhe Han, Bowen Du, Leilei Sun, Yanjie Fu, Yisheng Lv, and Hui Xiong. 2021. Dynamic and multi-faceted spatio-temporal deep learning for traffic speed forecasting. In *Proceedings of SIGKDD*. 547–555.
- [22] Xiaoxin He, Bryan Hooi, Thomas Laurent, Adam Perold, Yann LeCun, and Xavier Bresson. 2023. A generalization of vit/mlp-mixer to graphs. In *Proceedings of ICLR*. 12724–12745.
- [23] Bo Hui, Da Yan, Haiquan Chen, and Wei-Shinn Ku. 2021. Trajectory waveNet: A trajectory-based model for traffic forecasting. In *Proceedings of ICDM*. 1114–1119.
- [24] Jiawei Jiang, Chengkai Han, Wayne Xin Zhao, and Jingyuan Wang. 2023. Pdformer: Propagation delay-aware dynamic long-range transformer for traffic flow prediction. In *Proceedings of AAAI*. 4365–4373.
- [25] Xinke Jiang, Rihong Qiu, Yongxin Xu, Wentao Zhang, Yichen Zhu, Ruizhe Zhang, Yuchen Fang, Xu Chu, Junfeng Zhao, and Yasha Wang. 2024. RAGraph: A General Retrieval-Augmented Graph Learning Framework. *arXiv preprint arXiv:2410.23855* (2024).
- [26] Xinke Jiang, Dingyi Zhuang, Xianghui Zhang, Hao Chen, Jiayuan Luo, and Xiaowei Gao. 2023. Uncertainty quantification via spatial-temporal tweedie model for zero-inflated and long-tail travel demand prediction. In *Proceedings of CIKM*. 3983–3987.
- [27] Guangyin Jin, Yuxuan Liang, Yuchen Fang, Zezhi Shao, Jincai Huang, Junbo Zhang, and Yu Zheng. 2023. Spatio-temporal graph neural networks for predictive learning in urban computing: A survey. *IEEE Transactions on Knowledge and Data Engineering* (2023).
- [28] S Vasantha Kumar and Lelitha Vanajakshi. 2015. Short-term traffic flow prediction using seasonal ARIMA model with limited input data. *European Transport Research Review* (2015), 1–9.
- [29] Siqi Lai, Zhao Xu, Weijia Zhang, Hao Liu, and Hui Xiong. 2023. Large language models as traffic signal control agents: Capacity and opportunity. *arXiv preprint arXiv:2312.16044* (2023).
- [30] Zhichen Lai, Dalin Zhang, Huan Li, Christian S Jensen, Hua Lu, and Yan Zhao. 2023. Lightcts: A lightweight framework for correlated time series forecasting. *Proceedings of SIGMOD* (2023), 1–26.
- [31] Shiyong Lan, Yitong Ma, Weikang Huang, Wenwu Wang, Hongyu Yang, and Pyang Li. 2022. Dstagnn: Dynamic spatial-temporal aware graph neural network for traffic flow forecasting. In *Proceedings of ICLR*. 11906–11917.
- [32] Fuxian Li, Jie Feng, Huan Yan, Guangyin Jin, Fan Yang, Funing Sun, Depeng Jin, and Yong Li. 2023. Dynamic graph convolutional recurrent network for traffic prediction: Benchmark and solution. *ACM Transactions on Knowledge Discovery from Data* (2023), 1–21.
- [33] Rongfan Li, Ting Zhong, Xinke Jiang, Goce Trajcevski, Jin Wu, and Fan Zhou. 2022. Mining spatio-temporal relations via self-paced graph contrastive learning. In *Proceedings of SIGKDD*. 936–944.
- [34] Yaguang Li, Rose Yu, Cyrus Shahabi, and Yan Liu. 2018. Diffusion Convolutional Recurrent Neural Network: Data-Driven Traffic Forecasting. In *Proceedings of ICLR*.
- [35] Zhonghang Li, Lianghao Xia, Jiabin Tang, Yong Xu, Lei Shi, Long Xia, Dawei Yin, and Chao Huang. 2024. Urbangpt: Spatio-temporal large language models. In *Proceedings of SIGKDD*. 1–11.
- [36] Yuxuan Liang, Kun Ouyang, Junkai Sun, Yiwei Wang, Junbo Zhang, Yu Zheng, David Rosenblum, and Roger Zimmermann. 2021. Fine-grained urban flow prediction. In *Proceedings of WWW*. 1833–1845.
- [37] Yuxuan Liang, Yutong Xia, Songyu Ke, Yiwei Wang, Qingsong Wen, Junbo Zhang, Yu Zheng, and Roger Zimmermann. 2023. Airformer: Predicting nationwide air quality in china with transformers. In *Proceedings of AAAI*. 14329–14337.
- [38] Dachuan Liu, Jin Wang, Shuo Shang, and Peng Han. 2022. Msdr: Multi-step dependency relation networks for spatial temporal forecasting. In *Proceedings of SIGKDD*. 1042–1050.
- [39] Hangchen Liu, Zheng Dong, Renhe Jiang, Jiewen Deng, Jinliang Deng, Qunjun Chen, and Xuan Song. 2023. Spatio-temporal adaptive embedding makes vanilla transformer sota for traffic forecasting. In *Proceedings of CIKM*. 4125–4129.
- [40] Shuncheng Liu, Xu Chen, Ziniu Wu, Liwei Deng, Han Su, and Kai Zheng. 2022. HeGA: heterogeneous graph aggregation network for trajectory prediction in high-density traffic. In *Proceedings of CIKM*. 1319–1328.
- [41] Shuncheng Liu, Yuyang Xia, Xu Chen, Jiandong Xie, Han Su, and Kai Zheng. 2023. Impact-aware maneuver decision with enhanced perception for autonomous vehicle. In *Proceedings of ICDE*. 3255–3268.
- [42] Xu Liu, Yuxuan Liang, Chao Huang, Hengchang Hu, Yushi Cao, Bryan Hooi, and Roger Zimmermann. 2024. Reinventing Node-centric Traffic Forecasting for Improved Accuracy and Efficiency. In *Proceedings of ECML-PKDD*. 21–38.
- [43] Xu Liu, Yutong Xia, Yuxuan Liang, Junfeng Hu, Yiwei Wang, Lei Bai, Chao Huang, Zhengguang Liu, Bryan Hooi, and Roger Zimmermann. 2024. Largest: A benchmark dataset for large-scale traffic forecasting. In *Proceedings of NeurIPS*.
- [44] Ze Liu, Yutong Lin, Yue Cao, Han Hu, Yixuan Wei, Zheng Zhang, Stephen Lin, and Baining Guo. 2021. Swin transformer: Hierarchical vision transformer using shifted windows. In *Proceedings of ICCV*. 10012–10022.
- [45] Jiayuan Luo, Wentao Zhang, Yuchen Fang, Xiaowei Gao, Dingyi Zhuang, Hao Chen, and Xinke Jiang. 2024. Timeseries suppliers allocation risk optimization via deep black litterman model. *arXiv preprint arXiv:2401.17350* (2024).
- [46] Zhongjian Lv, Jiajie Xu, Kai Zheng, Hongzhi Yin, Pengpeng Zhao, and Xiaofang Zhou. 2018. Lc-rnn: A deep learning model for traffic speed prediction.. In *Proceedings of IJCAI*. 27.
- [47] Qian Ma, Zijian Zhang, Xiangyu Zhao, Haoliang Li, Hongwei Zhao, Yiqi Wang, Zitao Liu, and Wanyu Wang. 2023. Rethinking sensors modeling: Hierarchical information enhanced traffic forecasting. In *Proceedings of CIKM*. 1756–1765.
- [48] Chunghyun Park, Yoonwoo Jeong, Minsu Cho, and Jaesik Park. 2022. Fast point transformer. In *Proceedings of CVPR*. 16949–16958.
- [49] Cheonbok Park, Chunggi Lee, Hoyjin Bahng, Yunwon Tae, Seungmin Jin, Kihwan Kim, Sungahn Ko, and Jaegul Choo. 2020. ST-GRAT: A novel spatio-temporal

- graph attention networks for accurately forecasting dynamically changing road speed. In *Proceedings of CIKM*. 1215–1224.
- [50] Zezhi Shao, Zhao Zhang, Fei Wang, Wei Wei, and Yongjun Xu. 2022. Spatial-temporal identity: A simple yet effective baseline for multivariate time series forecasting. In *Proceedings of CIKM*. 4454–4458.
- [51] Zezhi Shao, Zhao Zhang, Wei Wei, Fei Wang, Yongjun Xu, Xin Cao, and Christian S Jensen. 2022. Decoupled dynamic spatial-temporal graph neural network for traffic forecasting. *Proceedings of VLDB* (2022), 2733–2746.
- [52] Robert F Sproull. 1991. Refinements to nearest-neighbor searching in k-dimensional trees. *Algorithmica* (1991), 579–589.
- [53] Qian Sun, Rui Zha, Le Zhang, Jingbo Zhou, Yu Mei, Zhiling Li, and Hui Xiong. 2024. CrossLight: Offline-to-Online Reinforcement Learning for Cross-City Traffic Signal Control. In *Proceedings of SIGKDD*. 2765–2774.
- [54] Peng-Shuai Wang. 2023. Octformer: Octree-based transformers for 3d point clouds. *ACM Transactions on Graphics (TOG)* (2023), 1–11.
- [55] Tianfu Wang, Liwei Deng, Chao Wang, Jianxun Lian, Yue Yan, Nicholas Jing Yuan, Qi Zhang, and Hui Xiong. 2024. COMET: NFT Price Prediction with Wallet Profiling. In *Proceedings of SIGKDD*. 5893–5904.
- [56] Xu Wang, Lianliang Chen, Hongbo Zhang, Pengkun Wang, Zhengyang Zhou, and Yang Wang. 2023. A Multi-graph Fusion Based Spatiotemporal Dynamic Learning Framework. In *Proceedings of WSDM*. 294–302.
- [57] Haomin Wen, Youfang Lin, Yutong Xia, Huaiyu Wan, Qingsong Wen, Roger Zimmermann, and Yuxuan Liang. 2023. Diffstg: Probabilistic spatio-temporal graph forecasting with denoising diffusion models. In *Proceedings of SIGSPATIAL*. 1–12.
- [58] Zonghan Wu, Shirui Pan, Guodong Long, Jing Jiang, Xiaojun Chang, and Chengqi Zhang. 2020. Connecting the dots: Multivariate time series forecasting with graph neural networks. In *Proceedings of SIGKDD*. 753–763.
- [59] Zonghan Wu, Shirui Pan, Guodong Long, Jing Jiang, and Chengqi Zhang. 2019. Graph wavenet for deep spatial-temporal graph modeling. In *Proceedings of IJCAI*. 1907–1913.
- [60] Chin-Chia Michael Yeh, Yujie Fan, Xin Dai, Uday Singh Saini, Vivian Lai, Prince Osei Aboagye, Junpeng Wang, Huiyuan Chen, Yan Zheng, Zhongfang Zhuang, et al. 2024. RPMixer: Shaking Up Time Series Forecasting with Random Projections for Large Spatial-Temporal Data. In *Proceedings of SIGKDD*.
- [61] Bing Yu, Haoteng Yin, and Zhanxing Zhu. 2018. Spatio-Temporal Graph Convolutional Networks: A Deep Learning Framework for Traffic Forecasting. In *Proceedings of IJCAI*. 3634–3640.
- [62] Xingtong Yu, Yuan Fang, Zemin Liu, Yuxia Wu, Zhihao Wen, Jianyuan Bo, Xinming Zhang, and Steven CH Hoi. 2024. Few-shot learning on graphs: from meta-learning to pre-training and prompting. *arXiv preprint arXiv:2402.01440* (2024).
- [63] Xingtong Yu, Zemin Liu, Yuan Fang, and Xinming Zhang. 2023. Learning to count isomorphisms with graph neural networks. In *Proceedings of AAAI*. 4845–4853.
- [64] Xingtong Yu, Zhenghao Liu, Yuan Fang, and Xinming Zhang. 2024. DyG-Prompt: Learning Feature and Time Prompts on Dynamic Graphs. *arXiv preprint arXiv:2405.13937* (2024).
- [65] Chuanpan Zheng, Xiaoliang Fan, Cheng Wang, and Jianzhong Qi. 2020. Gman: A graph multi-attention network for traffic prediction. In *Proceedings of AAAI*. 1234–1241.